Analysis of Flash-Induced FTIR Difference Spectra of the S-State Cycle in the Photosynthetic Water-Oxidizing Complex by Uniform ^{15}N and ^{13}C Isotope Labeling†

Takumi Noguchi*,‡ and Miwa Sugiura§

Institute of Materials Science, University of Tsukuba, Tsukuba, Ibaraki 305-8573, Japan, and Department of Applied Biological Chemistry, Faculty of Agriculture, Osaka Prefecture University, 1-1 Gakuen-cho, Sakai, Osaka, 599-8531 Japan

Received January 29, 2003; Revised Manuscript Received March 16, 2003

ABSTRACT: Protein bands in flash-induced Fourier transform infrared (FTIR) difference spectra of the S-state cycle of photosynthetic water oxidation were analyzed by uniform ^{15}N and ^{13}C isotopic labeling of photosystem II (PS II). The difference spectra upon first- to fourth-flash illumination were obtained with hydrated (for the 1800−1200 cm^{-1} region) or deuterated (for the 3500−3100 cm^{-1} region) films of unlabeled, ^{15}N-labeled, and ^{13}C-labeled PS II core complexes from *Thermosynechococcus elongatus*. Shifts of band frequencies upon ^{15}N and ^{13}C labeling provided the assignments of major peaks in the regions of 3450−3250 and 1700−1630 cm^{-1} to the NH stretches and amide I modes of polypeptide backbones, respectively, and the assignments of some of the peaks in the 1600−1500 cm^{-1} region to the amide II modes of backbones. Other prominent peaks in the latter region and most of the peaks in the 1450−1300 cm^{-1} region exhibited large downshifts upon ^{13}C labeling but were unchanged by ^{15}N labeling, and hence assigned to the asymmetric and symmetric COO^- stretching vibrations, respectively, of carboxylate groups in Glu, Asp, or the C-terminus. Peak positions corresponded well with each other among the first- to fourth-flash spectra, and most of the bands in the first- and/or second-flash spectra appeared with opposite signs of intensity in the third- and/or fourth-flash spectra. This observation indicates that the protein movements in the $S_1 \rightarrow S_2$ and/or $S_2 \rightarrow S_3$ transitions are mostly reversed in the $S_3 \rightarrow S_0$ and/or $S_0 \rightarrow S_1$ transitions, representing a catalytic role of the protein moieties of the water-oxidizing complex. Drastic structural changes in carboxylate groups over the S-state cycle suggest that the Asp and/or Glu side chains play important roles in the reaction mechanism of photosynthetic water oxidation.

Photosynthetic water oxidation is known to take place in the water-oxidizing complex (WOC),[1] which consists of a tetranuclear Mn cluster, located on the electron-donor side of photosystem II (PS II). The Mn cluster has been predicted to be coordinated mainly by the D1 protein from the data of site-directed mutagenesis (*1*), and this prediction was recently corroborated by X-ray crystallography of the PS II core complexes of cyanobacteria, *Thermosynechococcus elongatus* (formerly *Synechococcus elongatus*) (*2*) and *Thermosynechococcus vulcanus* (*3*). The reported electron-density map of the Mn cluster has a triangular shape, in which four manganese ions are positioned at the three corners and the center (*2, 3*). Also from the X-ray structure, the C-terminal carboxyl group of the D1 protein and the side chains of Asp-170, Glu-333 (or His-332), His-337, and Glu-189 (or His-190) were proposed to be coordinated to the Mn cluster (*3*), consistent with the results of site-directed mutagenesis (*1*). However, the detailed structure of the Mn cluster, including its ligands, indispensable cofactors of Ca^{2+} and Cl^-, and substrate water, is yet to be determined because of the relatively low resolution of the crystallographic data (3.7−3.8 Å) (*2, 3*).

In the WOC, two water molecules are oxidized as terminal electron donors in the photosynthetic electron transport chain, resulting in the formation of one molecular oxygen and four protons (for reviews, see refs *1*, *4*, and *5*). This reaction is known to occur though a so-called S-state cycle, a light-driven cycle of five intermediates designated S states (S_0-S_4) (*6, 7*). In this cycle, a single turnover flash transforms each S_i state ($i = 0-3$) into the next S_{i+1} state, and molecular oxygen is released in thermal relaxation of the S_4 state into the S_0 state. Since the S_1 state is the most dark stable, oxygen is evolved upon the first three flashes and then every four flashes. Although such a four-flash cycle of water oxidation is well established, its molecular mechanism remains largely unclarified.

As a spectroscopic method to investigate the structure and reactions of WOC, Fourier transform infrared spectroscopy (FTIR) has been employed in the past decade (*9*−*27*). FTIR spectra specific to WOC were selectively obtained in PS II complexes or membrane preparations by recording flash-induced difference spectra in the presence of an exogenous electron acceptor, ferricyanide (*9, 10*). Difference spectra

† This study was supported by a Grant-in-Aid for Scientific Research (No. 14540607) from the Ministry of Education, Culture, Sports, Science and Technology of Japan and by Special Research Project "NanoScience" at the University of Tsukuba.

* To whom correspondence should be addressed. Phone: +81-29-853-5126. Fax: +81-29-855-7440. E-mail: tnoguchi@ims.tsukuba.ac.jp.

‡ University of Tsukuba.

§ Osaka Prefecture University.

[1] Abbreviations: FTIR, Fourier transform infrared; IR, infrared; Mes, 2-(*N*-morpholino)ethanesulfonic acid; PS II, photosystem II; WOC, water-oxidizing complex.

10.1021/bi0341612 CCC: $25.00
Published on Web 05/03/2003

upon the $S_1 \rightarrow S_2$ transition (S_2/S_1 difference) were measured at a cryogenic temperature and analyzed by biochemical perturbations, with various global and selective amino acid isotope labeling. The presence of carboxylate (*10*−*14*) and His (*15*) ligands and structural coupling with a tyrosine residue (*16*) and an active water molecule (*17*) have been proposed. Chu et al. (*18*−*22*) also recorded the low-frequency region (<1000 cm^{-1}) of the S_2/S_1 FTIR spectra and detected the Mn−O−Mn bands of the Mn cluster. Recently, FTIR difference spectra obtained during the S-state cycle, representing all the flash-induced S-state transitions, were recorded independently by Hillier and Babcock (*23*) and by us (*24*, *25*) using PS II membrane fragments of spinach and PS II core complexes of *T. elongatus*, respectively. In these spectra, drastic reactions of protein moieties in WOC were revealed. The similar S-state measurement was extended to the water OH(D) region using moderately hydrated (or deuterated) PS II core complexes, and the reactions of water molecules during the S-state cycle were directly monitored by FTIR (*26*). Thus, FTIR spectroscopy that provides information about the structures and reactions of the protein moieties of WOC, the Mn cluster, and substrate water at the molecular level can be a powerful tool for investigating the molecular mechanism of water oxidation.

Despite such a fruitful method, however, analyses of the FTIR spectra of WOC are not straightforward because of the severe overlap of numerous bands and the complex behaviors of the peak positions upon changes in structures and molecular interactions. The first step toward interpretation of the spectra is thus assigning the observed bands to distinct chemical groups (e.g., individual amino acid side chains, backbones, and water) and then to the normal modes of their vibrations by various isotope labeling, taking account of the spectra of isolated chemical species (*28*−*30*), the empirical table of group frequencies (*31*), and normal-mode analyses by theoretical calculations. After solid assignments, information about structures and interactions of the chemical groups can be obtained by using marker bands with empirical and theoretical rules for interpretation (*32*−*39*).

In this study, protein bands in the flash-induced FTIR spectra of WOC during the S-state cycle have been analyzed by uniform ^{15}N and ^{13}C labeling of the core complexes from *T. elongatus*. These analyses allow assignments of the major bands in the difference spectra of the S-state transitions to the vibrational modes of protein backbones and side chains, providing insight into the reactions of protein moieties of WOC in the mechanism of photosynthetic water oxidation.

MATERIALS AND METHODS

T. elongatus, in which the carboxyl terminus of the CP43 subunit was genetically histidine-tagged, was cultured as described previously (*40*). Uniform ^{15}N labeling of cells was performed by culturing the cells in a medium including $K^{15}NO_3$, $Na^{15}NO_3$, and $^{15}NH_4Cl$ (Masstrace Inc., 99 at. % ^{15}N) instead of unlabeled nitrogen sources, and uniform ^{13}C labeling was done by using a medium in which 10 mM $NaH^{13}CO_3$ (Masstrace Inc., 99 at. % ^{13}C) and 20 mM Tricin were dissolved without bubbling of CO_2-enriched air. Oxygen-evolving PS II core complexes of *T. elongatus* were purified using Ni^{2+}-affinity column chromatography as described previously (*40*). The PS II core complexes were suspended in 10 mM Mes−NaOH (pH 6.0) containing 5 mM NaCl, 5 mM $CaCl_2$, and 0.06% *n*-dodecyl β-D-maltoside and concentrated to about 4.5 mg of Chl/mL using Microcon-100 (Amicon).

Moderately hydrated or deuterated films of the PS II core complexes in the presence of ferricyanide as an electron acceptor were prepared on a CaF_2 window (25 mm diameter × 3 mm) with humidity control using a 40% (v/v) glycerol/water solution, as reported previously (*25*, *26*). The sample temperature was kept at 10 °C by circulating cold water in a copper holder. Flash-induced FTIR difference spectra during the S-state cycle were measured as described in ref *25*, using a Bruker IFS-66/S spectrophotometer equipped with an MCT detector (InfraRed D316/8) and a Q-switched Nd:YAG laser (Quanta-Ray GCR-130; 532 nm; ∼7 ns fwhm). Briefly, after two preflashes and subsequent dark adaptation for 1 h, the sample was subjected to four consecutive flashes with 10-s intervals. Single-beam spectra (10 s scan) were recorded before and after each flash. The sample was then dark-adapted for 1 h, and this cycle was repeated up to 16 times for one sample. Difference spectra (after minus before the flash) were calculated for each flash, and the spectra for the same flash number were averaged. The final data for the hydrated and deuterated samples of the unlabeled complexes were the averages of 72 (1440 interferograms) and 120 (2400 interferograms) spectra, respectively, and those of the ^{15}N-labeled and ^{13}C-labeled complexes were the average of 16 (320 interferograms) spectra. All spectra were measured with a resolution of 4 cm^{-1}.

FTIR spectra of unlabeled and 1-^{13}C-labeled acetate were measured at room temperature using aqueous solutions (10%) in which CH_3COONa and $CH_3{}^{13}COONa$ (Masstrace Inc., 99% at. % ^{13}C), respectively, were dissolved. A water spectrum was subtracted from the acetate spectra to remove a broad HOH bending band around 1640 cm^{-1}.

RESULTS AND DISCUSSION

Amide I and II Bands of Protein Backbones. Figure 1 shows FTIR difference spectra (1770−1450 cm^{-1}) of flash-induced S-state transitions (a−d) of the WOC measured using hydrated films of the PS II core complexes from *T. elongatus* and original (not difference) FTIR absorption spectra of these PS II films (e). Red lines indicate the spectra of unlabeled complexes, and blue lines indicate those of uniformly ^{15}N-labeled (Figure 1A) and ^{13}C-labeled (Figure 1B) complexes. The first- (a), second- (b), third- (c), and fourth-flash (d) spectra virtually represent the structural changes in the $S_1 \rightarrow S_2$, $S_2 \rightarrow S_3$, $S_3 \rightarrow S_0$, and $S_0 \rightarrow S_1$ transitions, respectively (*24*, *25*). This wavenumber region includes typical bands of protein backbones: the amide I (C═O stretch) and amide II (NH bend coupled with CN stretch) bands in the 1700−1600 and 1600−1500 cm^{-1} regions, respectively (*32*, *33*). IR spectra of proteins in the mid-IR region generally consist of these two bands as a prominent structure, because of the number of amide groups of backbones much larger than those of individual side chains. In fact, the FTIR spectrum of the PS II core film (Figure 1A-e, red line) shows prominent amide I and amide II bands at 1657 and 1548 cm^{-1}, respectively. Upon uniform ^{15}N labeling (Figure 1A-e, blue line) of the core complexes, the amide I band was slightly downshifted by ∼1 cm^{-1}, due to a small coupling with the

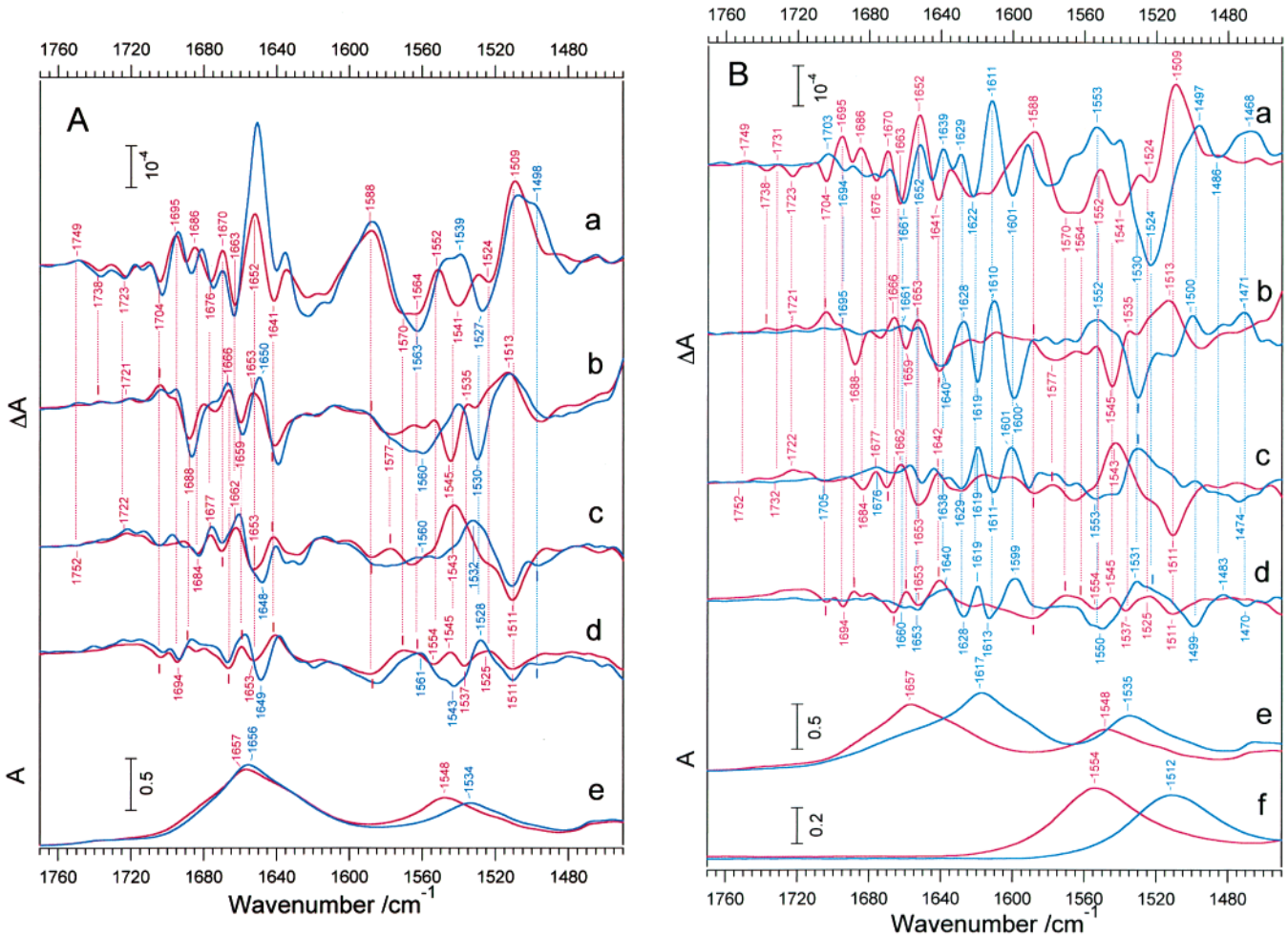

FIGURE 1: (A) FTIR difference spectra (1770−1450 cm^{-1}) of the WOC upon (a) first-, (b) second-, (c) third-, and (d) fourth-flash illumination of hydrated films of unlabeled (red lines) and uniformly ^{15}N-labeled (blue lines) PS II core complexes from *T. elongatus*, and (e) their FTIR absorption spectra. (B) FTIR difference spectra (1770−1450 cm^{-1}) of the WOC upon (a) first-, (b) second-, (c) third-, and (d) fourth-flash illumination of hydrated films of unlabeled (red lines) and uniformly ^{13}C-labeled (blue lines) PS II core complexes from *T. elongatus*, and (e) their FTIR absorption spectra. (f) FTIR spectra (1770−1450 cm^{-1}) of unlabeled (red line) and 1-^{13}C-labeled ($CH_3{}^{13}COO^-$) (blue line) acetate in aqueous solutions. The spectra of PS II core complexes were measured at 10 °C in the presence of ferricyanide as an electron acceptor. The scale bars are for the spectra of the unlabeled complexes, and the spectra of ^{15}N- and ^{13}C-labeled complexes were roughly scaled to adjust the intensities. In the acetate spectra, a broad water band around 1640 cm^{-1} was removed by subtraction of the water spectrum from the original spectra.

NH bending vibration, while the amide II band showed a larger downshift by 14 cm^{-1}, consistent with the assignment of the latter band to the NH and CN vibrations. In contrast, upon ^{13}C labeling (Figure 1B-e, blue line), the amide I band showed a significant downshift by 40 cm^{-1}, while the amide II band moderately downshifted by 13 cm^{-1}, similar to the extent of the shift due to ^{15}N labeling.

If some structural changes occur in the protein backbones upon S-state transitions, flash-induced difference spectra should show bands in the amide I and II regions. Prominent bands were, indeed, observed in these regions in all the first- to fourth-flash spectra (Figure 1A-a−d, red lines). Peaks in the complex features in the 1700−1630 cm^{-1} region showed large downshifts by ∼40 cm^{-1} upon ^{13}C labeling (Figure 1B-a−d, blue lines), whereas ^{15}N labeling induced only slight downshifts by 1−3 cm^{-1} (Figure 1A-a−d, blue lines). For example, peaks at 1695/1686/1670/1663/1652/1641 cm^{-1} in the first-flash spectrum shifted to 1652/1639/1629/1622/1611/1601 cm^{-1} upon ^{13}C labeling, those at 1688/1666/1659/1653/1641 cm^{-1} in the second-flash spectrum to 1640/1628/1619/1610/1600 cm^{-1}, those at 1670/1662/1653/1642 cm^{-1} in the third-flash spectrum to 1629/1619/1611/1601 cm^{-1}, and those at 1670/1659/1653/1641 cm^{-1} in the fourth-flash spectrum to 1628/1619/1613/1599 cm^{-1} (Figure 1B-a−d). Thus, most of the prominent peaks in the 1700−1630 cm^{-1} region are consistent with the assignments to the amide I bands.

Some contributions of side chains to this region of 1700−1630 cm^{-1} are also possible. IR bands of the side groups of amino acids in the mid-IR region have been extensively studied (*28*−*30*). Among them, prominent bands that appear in the 1700−1630 cm^{-1} region are the C═O stretches of the amide groups of Gln and Asn at 1690−1660 cm^{-1}, the asymmetric and symmetric stretches of a guanidinium group ($CN_3H_5^+$) of Arg at ∼1675 and ∼1635 cm^{-1}, respectively, and the NH_3^+ deformation of Lys at ∼1630 cm^{-1}. The C═O bands of Gln and Asn should show ^{13}C and ^{15}N effects similar to those exhibited by the amide I bands, and thus, contributions of these side chains are not distinguishable from the amide I bands in this study. By contrast, the $CN_3H_5^+$ stretching bands of Arg shows relatively large downshifts by 6−9 cm^{-1} due to ^{15}N labeling (*41*), which was not explicitly observed in the flash-induced spectra, and hence

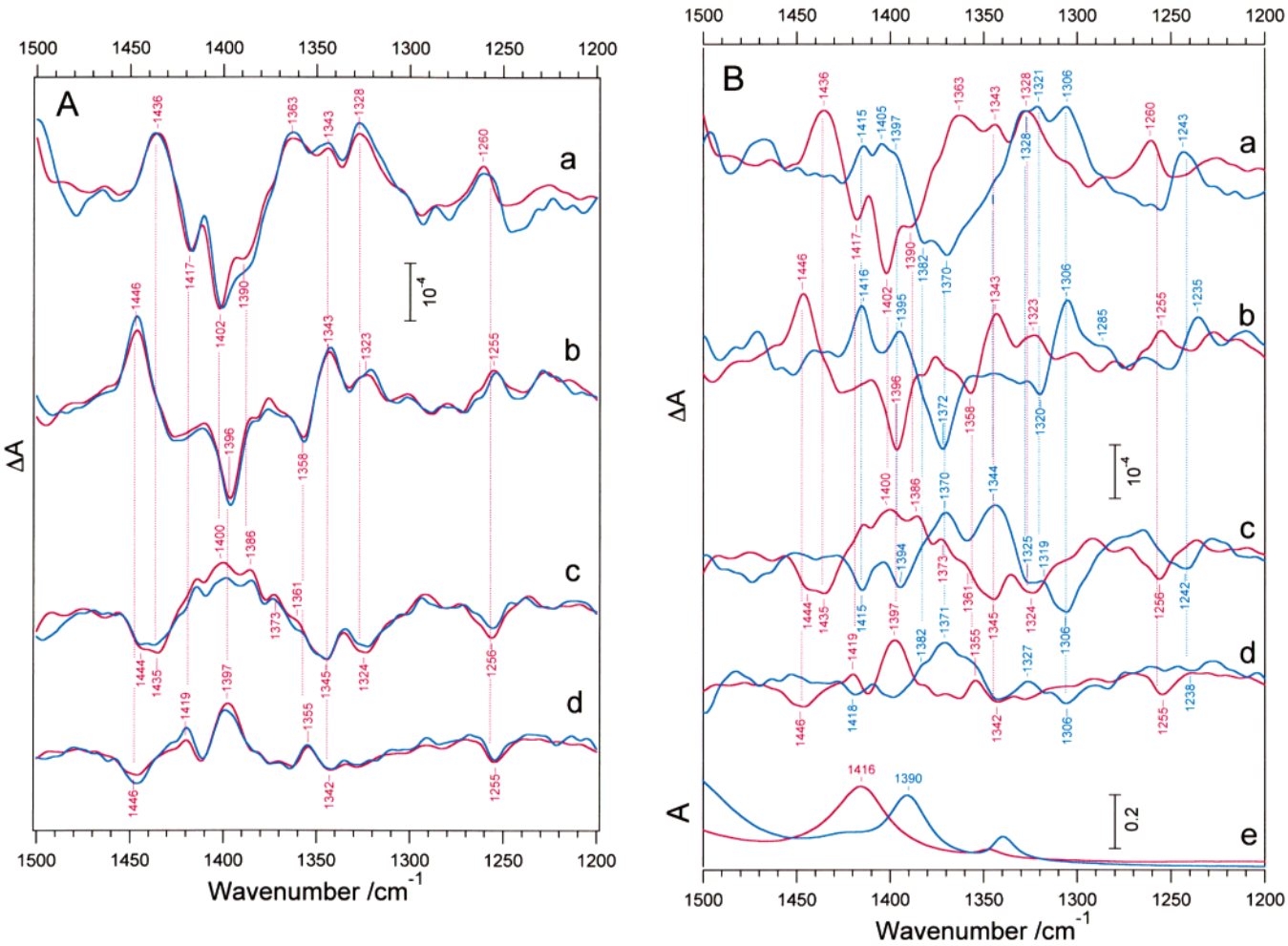

FIGURE 2: (A) FTIR difference spectra (1500−1200 cm^{-1}) of the WOC upon (a) first-, (b) second-, (c) third-, and (d) fourth-flash illumination of hydrated films of unlabeled (red lines) and uniformly ^{15}N-labeled (blue lines) PS II core complexes from *T. elongatus*. (B) FTIR difference spectra (1500−1200 cm^{-1}) of the WOC upon (a) first-, (b) second-, (c) third-, and (d) fourth-flash illumination of hydrated films of unlabeled (red lines) and uniformly ^{13}C-labeled (blue lines) PS II core complexes from *T. elongatus*. (e) FTIR spectra (1500−1200 cm^{-1}) of unlabeled (red line) and 1-^{13}C-labeled ($CH_3{}^{13}COO^-$) (blue line) acetate in aqueous solutions. Measurement conditions and the scale bars are the same as those for Figure 1.

only a minor contribution of Arg, if any, might be present in this region. The presence of a Lys NH_3^+ band is less likely, because there is only one Lys residue (Lys-310), which is not a conserved amino acid residue, in the lumenal side of the D1 protein of *T. elongatus* (*42*). Note that the intensity of the 1652 cm^{-1} band at the first flash significantly increased upon ^{15}N labeling (Figure 1A-a). This might be the consequence of the mixed effects of shifts and intensity changes in some ^{15}N-sensitive bands. However, it is also possible that this is due to a subtle difference in the sample condition between the ^{15}N-labeled and unlabeled core films, because the amide I intensities were previously shown to be highly sensitive to the extent of hydration (*25*).

Some of the prominent peaks in the 1600−1500 cm^{-1} region showed clear downshifts upon ^{15}N labeling. For example, bands at 1541 (first flash), 1545 (second flash), 1543 (third flash), and 1545 (fourth flash) cm^{-1} shifted down to 1527, 1530, 1532, and 1528 cm^{-1}, respectively, by 11−17 cm^{-1} (Figure 1Aa-d). Also, a part of the 1570 cm^{-1} bands at the first and fourth flashes seems to shift to 1563 and 1561 cm^{-1}, respectively, and the 1577 cm^{-1} bands at the second and third flashes shift to ∼1560 cm^{-1}. In addition, some contributions of the bands at 1509−1513 cm^{-1} in the first to fourth flash spectra shift to ∼1498 cm^{-1}. Upon ^{13}C labeling, these ^{15}N-sensitive bands all shifted down to similar extents (Figure 1B-a−d). These isotope effects resemble those of the amide II bands in the absorption spectra of the PS II core films (Figure 1A-e and B-e), consistent with the assignments of the above bands to the amide II modes. When amide groups are deuterated, the amide II bands downshift by about 100 cm^{-1}. However, our previous data (*26*) showed that the above bands did not drastically change after deuteration of the PS II film, except for some intensity decreases in the 1541 and 1513 cm^{-1} bands in the first and second flashes, respectively, and additionally no new prominent peaks appeared in the 1400−1500 cm^{-1} region. This observation indicates that amide groups in the polypeptide chains perturbed during the S-state cycle are present mostly in hydrophobic environments.

C═O Stretching Bands of Carboxylate Groups. Carboxylate groups generally exhibit strong IR bands in the regions of 1600−1500 and 1450−1300 cm^{-1}, arising from the asymmetric and symmetric COO^- stretching vibrations (*34*). Acetate, the simplest model compound of the carboxylate side chains of Asp and Glu, in aqueous solution showed an asymmetric stretching band at 1554 cm^{-1} (Figure 1B-f, red line) and a symmetric stretching band at 1416 cm^{-1} (Figure 2B-e, red line). These bands downshifted to 1512 (Figure

1B-f, blue line) and 1390 cm^{-1} (Figure 2B-e, blue line) by 42 and 26 cm^{-1}, respectively. Thus, although the wavenumber region of asymmetric COO^- stretches overlaps that of amide II bands, the asymmetric COO^- bands show isotope effects totally different from the amide II bands: they are insensitive to ^{15}N labeling but exhibit a large downshift of $\sim$40 cm^{-1} upon ^{13}C labeling.

In the 1600−1500 cm^{-1} region of flash-induced difference spectra, there are bands that were unchanged by ^{15}N labeling but showed drastic downshifts upon ^{13}C labeling. For instance, the bands at 1588 cm^{-1} that appear in all the difference spectra were insensitive to ^{15}N labeling (Figure 1A-a−d) but all downshifted by 35−38 cm^{-1}, to 1553−1550 cm^{-1}, upon ^{13}C labeling (Figure 1B-a−d). Bands at 1570−1564 cm^{-1} in the first- and fourth-flash spectra, which include some of the amide II contributions (see above), seemed to downshift to the bands around 1524 cm^{-1} upon ^{13}C labeling. In addition, bands at 1513−1509 cm^{-1} in all the flash-induced spectra, which also include contributions from amide II bands, shifted by 37−42 cm^{-1}, to 1474−1468 cm^{-1}. Thus, these bands are most probably attributed to the asymmetric COO^- stretching vibrations of Asp, Glu, or the C-terminus. It is noted that the COO^- band that upshifted upon deuteration in the S_2/S_1 spectrum (*11*, *26*), and hence was interpreted as interacting with a water molecule (*11*, *43*), is included in the bands at 1570−1564 cm^{-1}.

The behaviors of the bands in the symmetric COO^- region were much simpler. All the prominent bands in the 1450−1300 cm^{-1} region were unaffected by ^{15}N labeling (Figure 2A) but significantly downshifted upon ^{13}C labeling (Figure 2B-a−d). The bands were shifted down by $\sim$30 cm^{-1}, preserving the basic spectral features, although the detailed band shapes were altered because of the different extents of shift (20−45 cm^{-1}), depending on the individual bands (Figure 2B-a−d). For this reason, correspondences between unlabeled and ^{13}C-labeled bands were sometimes not easy to find, whereas many bands clearly corresponded to each other. Bands at 1417/1402/1328 cm^{-1} in the first-flash spectrum shift to 1382/1370/1306 cm^{-1} upon ^{13}C labeling, and bands at 1446/1396/1358/1343 cm^{-1} in the second-flash spectrum shift to 1416/1372/1320/1306 cm^{-1} (Figure 2B-a,b). Also, bands at 1444/1435/1400/1386/1324 cm^{-1} in the third-flash spectrum shift to 1415/1394/1370/1344/1306 cm^{-1}, and bands at 1446/1419/1397/1355/1342 cm^{-1} in the fourth-flash spectrum shift to 1418/1382/1371/1327/1306 cm^{-1} (Figure 2B-c,d). Thus, major bands in the 1450−1300 cm^{-1} region are mostly assigned to the symmetric COO^- stretches, which are coupled to the asymmetric vibrations in the 1600−1500 cm^{-1} region.

When a caroxylate group is protonated, the C═O stretching band of carboxylic acid (COOH) occurs typically in the 1790−1700 cm^{-1} region (*28*, *29*, *31*). Since no other vibrations of side chians and polypeptide backbones show bands in this region (*28*, *29*), the assignment is rather straightforward. Only minor peaks were observed in this region in all the flash-induced spectra (Figure 1A-a−d, red lines). These peaks were basically insensitive to ^{15}N labeling (within 1 cm^{-1}) (Figure 1A-a−d, blue lines) but shifted down by 40−50 cm^{-1} upon ^{13}C labeling (Figure 1B-a−d, blue lines), consistent with the COOH assignments. Bands at 1704 cm^{-1} (at the first, second, and fourth flashes), on the border between the COOH and amide I regions, are difficult to assign unambiguously to either mode. Note that broad positive baselines in this region in the second- to fourth-flash spectra are due to nonspecific COOH groups of the PS II proteins by pH decrease upon proton release in the S-state transitions (*24*). Insensitivity of the COOH peaks to deuteration (*26*) indicates the hydrophobic environments around the COOH groups. In addition, weak intensities of the COOH bands compared with, for example, the COO^- bands indicate that these bands appeared in the FTIR difference spectra after subtle changes in the interactions or the electrostatic environment, or only partial protonation/deprotonation reactions, if any. Efficient protonation/deprotonation of COO^-/COOH groups was not observed, at least between the stable S-state intermediates (S_0-S_3). Needless to say, this result by no means excludes the mechanism in which Asp or Glu side chains function as proton-transfer mediators by the protonation/deprotonation reactions during the S-state transitions.

Medium-intensity bands are present at 1260−1255 cm^{-1}, frequencies lower than the symmetric COO^- stretching region, with positive intensities in the first and second flashes and negative intensities in the third and fourth flashes (Figure 2A). The peak frequencies were unchanged by ^{15}N labeling (Figure 2A, blue lines) but downshifted by 14−20 cm^{-1} upon ^{13}C labeling (Figure 2B, blue lines), indicating that the signals arise from a vibration including a carbon atom(s) but no nitrogen atom. One of the plausible assignments of these bands is the COH deformation of the hydroxyl group in Ser or Thr. The COH deformation mode of ethanol shows a strong band at $\sim$1240 cm^{-1} in an Ar matrix as a monomer (*44*) and at an upshifted frequency of $\sim$1300 cm^{-1} as a proton donor in a dimer (*45*). The peak frequencies at 1260−1255 cm^{-1} in the flash-induced spectra suggest a weak H-bonding interaction. Although these peaks were insensitive to deuteration of the PS II film (*26*), this may mean a hydrophobic environment around the COH group. The COH deformation/CO stretching vibrations of Tyr are also located in this region (*39*, *46*). However, the positive peak at 1260 cm^{-1} in the S_2/S_1 spectrum was previously shown to be unaffected by ring-4-^{13}C-Tyr labeling of the PS II core complexes from *Synechocystis* 6803 (*16*). In the latter study, the Tyr band was suggested to be present at 1254 cm^{-1}, with a negative intensity superimposing the positive 1260 cm^{-1} band in the S_2/S_1 spectrum (*16*). Further studies using selective isotope labeling of Tyr are necessary to identify the Tyr bands in the flash-induced S-state spectra of *T. elongatus*.

High-Frequency Region of Deuterated PS II Core Complexes. Flash-induced difference spectra in the high-frequency region of proteins were recorded using deuterated PS II core films to avoid a severe overlap of water OH absorption that significantly increases the noise level (*25*, *26*). The spectra in the 3500−3080 cm^{-1} region are presented in Figure 3A-a−d (unlabeled and ^{15}N-labeled) and B-a−d (unlabeled and ^{13}C-labeled). FTIR absorption spectra of the deuterated core films are also shown in Figure 3A-e and B-e. A major feature in this region is provided by the NH stretching bands of polypeptide backbones, along with minor contributions from the OH and NH stretches of side chains (*31*). Because of the deuterated samples, bands observed in this region arise from nonexchangeable groups of backbones and side chains, and the bands of exchangeable groups shift to the ND and OD stretching region of 2800−2200 cm^{-1}. It was previously

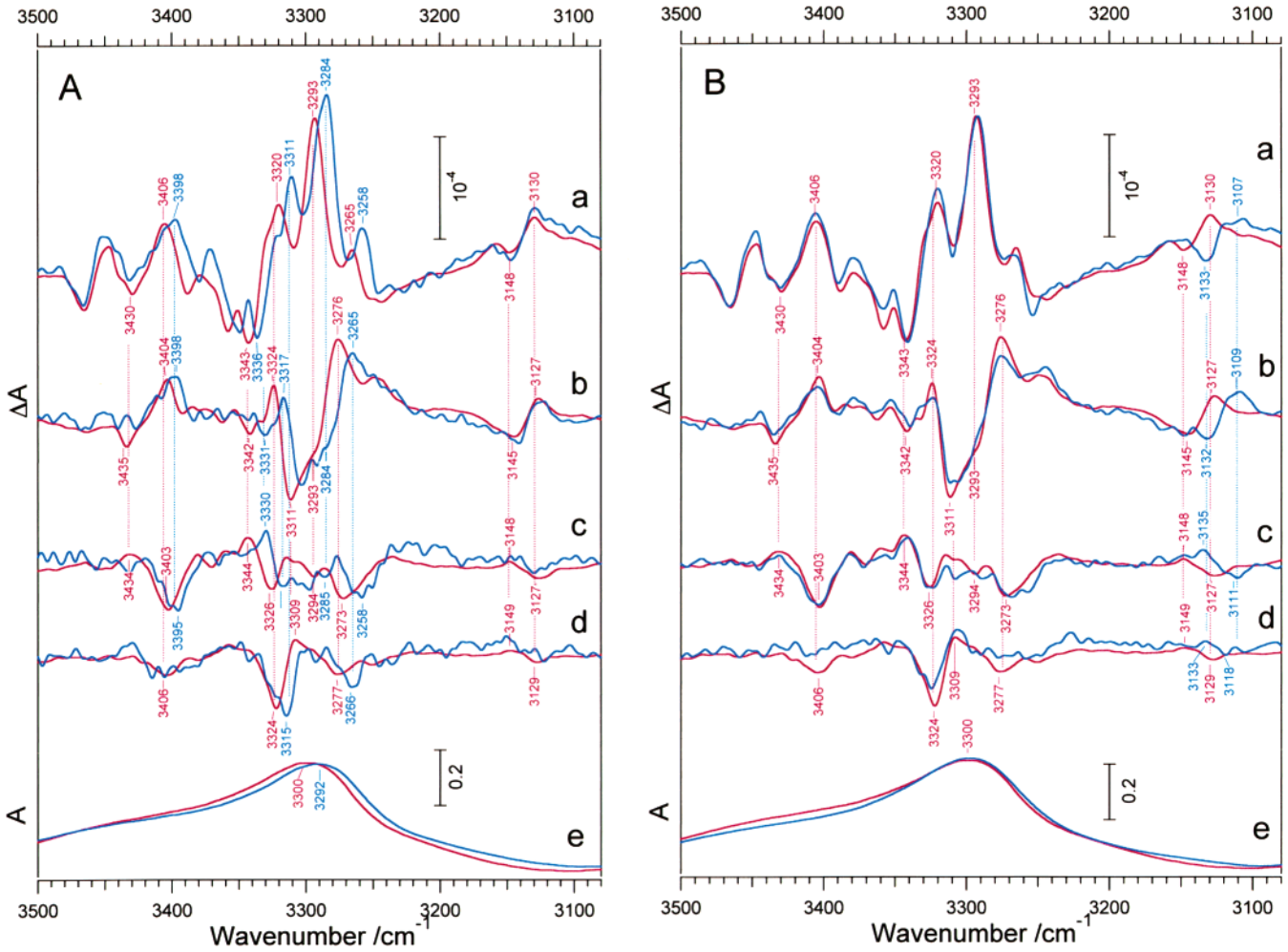

FIGURE 3: (A) FTIR difference spectra (3500−3080 cm^{-1}) of the WOC upon (a) first-, (b) second-, (c) third-, and (d) fourth-flash illumination of deuterated films of unlabeled (red lines) and uniformly ^{15}N-labeled (blue lines) PS II core complexes from *T. elongatus*, and (e) their FTIR absorption spectra. (B) FTIR difference spectra (3500−3080 cm^{-1}) of the WOC upon (a) first-, (b) second-, (c) third-, and (d) fourth-flash illumination of deuterated films of unlabeled (red lines) and uniformly ^{13}C-labeled (blue lines) PS II core complexes from *T. elongatus*, and (e) their FTIR absorption spectra. Measurement conditions and the scale bars are the same as those for Figure 1.

shown, however, that most of the bands were left in this protonated region in the S-state spectra, indicating that a large portion of the protein moieties that are active during the S-state cycle are in rather hydrophobic environments (*26*). The absorption spectrum of the deuterated film showed a peak at 3300 cm^{-1}, which downshifted by 8 cm^{-1} upon ^{15}N labeling (Figure 3A-e) but was unchanged by ^{13}C labeling (Figure 3B-e). The 8 cm^{-1} downshift is in agreement with the theoretical value of the ^{15}N shift of an isolated NH vibration, supporting the assignment to the amide NH stretches of backbones.

In the flash-induced difference spectra, most of the bands in the 3450−3250 cm^{-1} region also shifted down by ∼8 cm^{-1} upon ^{15}N labeling (Figure 3A-a−d, blue lines) without shifts upon ^{13}C labeling (Figure 3B, blue lines), suggesting that these bands arise from the NH vibrations of the protein backbones that are coupled to the structural changes in each S-state transition. Typical features are the peaks at 3406−3403 (in the first to fourth flashes), 3344−3342 (in the first to third flashes), 3326−3320 (in the first to fourth flashes), 3294−3293 (in the first to third flashes), and 3277−3273 cm^{-1} (at the second to fourth flashes) (Figure 3A-a−d). The NH stretches of Gln, Asn, and Arg side chains can be included in the ^{15}N-sensitive bands in this region.

Notable peaks were observed as differential signals at 3149−3145/3130−3127 cm^{-1} in all the flash-induced spectra. These peaks were unchanged by ^{15}N labeling (Figure 3A-a−d) but shifted down by ∼15 cm^{-1} upon ^{13}C labeling (Figure 3B-a−d), indicative of the vibrations including carbon atoms without nitrogen atoms. These vibrational frequencies are not in agreement with the CH stretching frequencies of methyl (CH_3−) and methylene (−CH_2−) groups (2975−2840 cm^{-1}), nor with those of aromatic groups (3080−3010 cm^{-1}) (*31*). The frequencies best match the CH stretches of an imidazole group of His. FTIR and Raman measurements of 4-methyimidazole, a simple model compound of a His side chain, showed CH stretching bands at 3165−3112 cm^{-1} in the neutral N1- or N3-protonated forms (*36*). However, the observed ^{13}C downshift by ∼15 cm^{-1} is a little too large, compared with the theoretical value of ∼9 cm^{-1} for an isolated CH vibration. The possibility of overtones or combinations of some lower-frequency vibrations consisting of only carbon, oxygen, and hydrogen atoms for the origin of this signal cannot be excluded.

CONCLUDING REMARKS

The frequencies, intensity signs (positive or negative), shifts resulting from ^{15}N and ^{13}C labeling, and probable

Table 1: Vibrational Frequencies (cm^{-1}) of Bands in the 1750−1200 cm^{-1} Region of FTIR Difference Spectra of the Flash-Induced S-State Transitions in Hydrated PS II Core Complexes and Shifts upon Uniform ^{15}N and ^{13}C Labeling

first flash ($S_1\rightarrow S_2$)			second flash ($S_2\rightarrow S_3$)			third flash ($S_3\rightarrow S_0$)			fourth flash ($S_0\rightarrow S_1$)			
unlabeled[a]	$\Delta^{15}N$[b]	$\Delta^{13}C$[c]	unlabeled	$\Delta^{15}N$	$\Delta^{13}C$	unlabeled	$\Delta^{15}N$	$\Delta^{13}C$	unlabeled	$\Delta^{15}N$	$\Delta^{13}C$	assignments[d]
1749(+)		−46				1752(−)		−47				COOH C═O st
1738(−)		−44	1738(+)		−43							COOH C═O st
1723(−)		−41	1721(+)		−42	1722(+)		−46				COOH C═O st
1704(−)	−1	−43	1704(+)		−43				1704(−)	−1	−44	COOH C═O st or amide I
1695(+)	−1	−43							1694(−)	−1	−41	amide I
			1688(−)	−2	−48				1688(+)	−2	−48	amide I
1686(+)	−4	−47				1684(−)	−1	−46				amide I
1676(−)	−1	−43				1677(+)	−1	−42				amide I
1670(+)	0	−41				1670(−)	0	−41				amide I
			1666(+)		−38				1666(−)		−38	amide I
1663(−)		−41				1662(+)	−2	−43				amide I
			1659(−)		−40				1659(+)	−1	−40	amide I
1652(+)	−1	−41	1653(+)	−3	−43	1653(−)	−5	−42	1653(−)	−4	−40	amide I
1641(−)	−1	−40	1641(−)	−2	−41	1642(+)	−2	−39	1641(+)	−3	−42	amide I
1588(+)		−35	∼1588(+)		−36	1588(−)		−35	1588(−)		−38	as COO^- st
			1577(−)	−17	−12	1577(+)	−17	−12				amide II
1570(−)	−7	−8							1570(+)	−9	−7	amide II
1570(−)		−40/−46							1570(+)		−40/−46	as COO^- st
1564(−)		−34/−40							1564(−)		−33/−40	as COO^- st
1552(+)	−13	−11							1554(−)	−11	∼−12	amide II
1541(−)	−14	−11	1545(−)	−15	−15	1543(+)	−11	−13	1545(+)	−17	−14	amide II
			1535(+)		−35				1537(−)		−38	as COO^- st
1524(−)		−38							1525(+)		−42	as COO^- st
1509(+)	−11	−12	1513(+)		−13	1511(+)	−13		1511(−)	−15	−12	amide II
1509(+)		−41	1513(+)		−42	1511(+)		−37	1511(−)		−41	as COO^- st
			1446(+)		−30	1444(−)		−29	1446(−)		−28	s COO^- st
1436(+)		−31/−39				1435(−)		−41				s COO^- st
1417(−)		−35							1419(+)		−37	s COO^- st
1402(−)		−32				1400(+)		−30				s COO^- st
			1396(−)		−24				1397(+)		−26	s COO^- st
1390(−)		∼ −40				1386(+)		−42				s COO^- st
1363(+)		−35/−42										s COO^- st
			1358(−)		−38	∼1361(+)		−42	1355(+)		−28	s COO^- st
1343(+)		−22/−34				1345(−)		−20/−39				s COO^- st
			1343(−)		−37				1342(−)		−36	s COO^- st
1328(+)		−22				1324(−)		−18				s COO^- st
1260(+)		−17	1255(+)		−20	1256(−)		−14	1255(−)		−17	COH def ?

[a] The plus and minus signs in parentheses indicate positive and negative intensities, respectively. [b] Shifts upon uniform ^{15}N labeling. [c] Shifts upon uniform ^{13}C labeling. [d] Abbreviations for assignments: st, stretching; def, deformation; s, symmetric; as, asymmetric.

Table 2: Vibrational Frequencies (cm^{-1}) of Bands in the High-Frequency Region of FTIR Difference Spectra of the Flash-Induced S-State Transitions in Deuterated PS II Core Complexes and Shifts upon Uniform ^{15}N and ^{13}C Labeling

first flash ($S_1\rightarrow S_2$)			second flash ($S_2\rightarrow S_3$)			third flash ($S_3\rightarrow S_0$)			fourth flash ($S_0\rightarrow S_1$)			
unlabeled[a] (in D_2O)	$\Delta^{15}N$[b]	$\Delta^{13}C$[c]	unlabeled (in D_2O)	$\Delta^{15}N$	$\Delta^{13}C$	unlabeled (in D_2O)	$\Delta^{15}N$	$\Delta^{13}C$	unlabeled (in D_2O)	$\Delta^{15}N$	$\Delta^{13}C$	assignments[d]
3406(+)	−8		3404(+)	−6		3403(−)	−8		3406(−)			backbone NH st
3343(−)	−7		3342(−)	−11		3344(+)	−14					backbone NH st
3320(+)	−9		3324(+)	−7		3326(−)	−9		3324(−)	−9		backbone NH st
3293(+)	−9		3293(−)	−9		3294(−)	−9					backbone NH st
			3276(+)	−11		3273(−)	−15		3277(−)	−11		backbone NH st
3148(−)		−15	3145(−)		−13	3148(+)		−13	3149(+)		−16	His CH st, or over/comb?
3130(+)		−23	3127(+)		−18	3127(−)		−16	3129(−)		−13	His CH st, or over/comb?

[a] The plus and minus signs in parentheses indicate positive and negative intensities, respectively. [b] Shifts upon uniform ^{15}N labeling. [c] Shifts upon uniform ^{13}C labeling. [d] Abbreviations for assignments: st, stretching; over, overtone; comb, combination.

assignments of FTIR bands in the flash-induced spectra of the S-state cycle are summarized in Tables 1 and 2 for the mid-IR (1770−1200 cm^{-1}) and high-frequency (3500−3080 cm^{-1}) regions, respectively. Major bands at 3450−3250 and 1700−1630 cm^{-1} were assigned to the NH stretches and amide I modes of polypeptide backbones, respectively, and some of the bands in the 1600−1500 cm^{-1} region that were sensitive to both ^{15}N and ^{13}C labeling were attributed to the amide II modes. The other major bands in the latter region and all the prominent bands at 1450−1300 cm^{-1}, which were sensitive only to ^{13}C labeling, were assigned to the asymmetric and symmetric COO^- stretching vibrations, respectively, of carboxylate groups in Glu, Asp, or the C-terminus. Minor peaks at 1750−1700 cm^{-1} were attributed to the C═O stretches of the protonated form (COOH) of these groups. The peaks at 3150−3125 cm^{-1} may arise from the CH stretches of a His side chain or overtones/combinations of some nitrogen-free vibrations, and the medium-intensity peaks at 1260−1255 cm^{-1} may be from the COH deformations of Ser or Thr.

Because of the enzymatic role of the WOC proteins, any movements and reactions of protein backbones and side chains should return back to the initial state during the oxygen-evolving S-state cycle. Indeed, peak positions correspond well to each other among the first- to fourth-flash spectra (Figures 1−3, Tables 1 and 2), which is somewhat surprising, considering the severe overlap of a number of bands. It was also shown that most of the bands of backbones and side chains in the first- and/or second-flash spectra appeared with opposite intensities in the third- and/or fourth-flash spectra (Figures 1−3, Tables 1 and 2). For instance, prominent peaks in the amide I region at 1663/1652/1641 and 1659/1653/1641 cm^{-1} with a negative/positive/negative (−/+/−) intensity pattern in the first- and second-flash spectra, respectively, correspond to the peaks at 1662/1653/1642 and 1659/1653/1641 cm^{-1} with an opposite +/−/+ pattern in the third- and fourth-flash spectra, respectively (Figure 1, Table 1). Also, typical amide II bands at 1545−1541 cm^{-1} show negative intensities in the first and second flashes but positive intensities in the third and fourth flashes (Figure 1A, Table 1). In addition, prominent negative bands at 1402 and 1396 cm^{-1} in the first- and second-flash spectra, respectively, which were assigned to the symmetric COO^- stretching vibrations, correspond to positive counter bands at 1400 and 1397 cm^{-1} in the third- and fourth-flash spectra, respectively (Figure 2, Table 1). Such observations suggest that the structural changes and reactions in the protein moieties of WOC during the $S_1 \rightarrow S_2$ and/or $S_2 \rightarrow S_3$ transitions are reversed during the $S_3 \rightarrow S_0$ and/or $S_0 \rightarrow S_1$ transitions. This characteristic of the protein bands is, however, in contrast with the behavior of the water OH(D) bands: major OH(D) peaks in flash-induced spectra showed different frequencies with mostly negative intensities, representing consumption of substrate water during the S-state cycle (*26*). Drastic structural changes in carboxylate groups over the S-state cycle indicate that Asp and/or Glu side chains play important roles in the reaction mechanism of water oxidation, such as by working as proton-transfer mediators or changing the structure or reactivity of the Mn cluster by altering the coordination structures, which is known as the "carboxylate shift" (*47*).

Further analyses of the FTIR difference spectra of the S-state cycle using selective isotope labeling of amino acid side chains and site-directed mutagenesis will provide decisive assignments of the bands to individual residues and then a clearer view of their roles in the molecular mechanism of photosynthetic water oxidation.

REFERENCES

1. Debus, R. J. (1992) *Biochim. Biophys. Acta 1102*, 269−352.
2. Zouni, A., Witt, H. T., Kern, J., Fromme, P., Krauss, N., Saenger, W., and Orth, P. (2001) *Nature 409*, 739−743.
3. Kamiya, N., and Shen, J.-R. (2003) *Proc. Natl. Acad. Sci. U.S.A. 100*, 98−103.
4. Britt, R. D. (1996) in *Oxygenic Photosynthesis: The Light Reactions* (Ort, D. R., and Yocum, C. F., Eds.) pp 137−164, Kluwer, Dordrecht, The Netherlands.
5. Yachandra, V. K., Sauer, K., and Klein, M. P. (1996) *Chem. Rev. 96*, 2927−2950.
6. Joliot, P., Barbieri, G., and Chabaud, R. (1969) *Photochem. Photobiol. 10*, 309−329.
7. Kok, B., Forbush, B., and McGloin, M. (1970) *Photochem. Photobiol. 11*, 457−475.
8. Yachandra, V. K., DeRose, V. J., Latimer, M. J., Mukerji, I., Sauer, K., and Klein, M. P. (1993) *Science 260*, 675−679.
9. Noguchi, T., Ono, T., and Inoue, Y. (1992) *Biochemistry 31*, 5953−5956.
10. Noguchi, T., Ono, T., and Inoue, Y. (1995) *Biochim. Biophys. Acta 1228*, 189−200.
11. Noguchi, T., Ono, T., and Inoue, Y. (1995) *Biochim. Biophys. Acta 1232*, 59−66.
12. Kimura, Y., and Ono, T. (2001) *Biochemistry 40*, 14061−14068.
13. Kimura, Y., Hasegawa, K., and Ono, T. (2002) *Biochemistry 41*, 5844−5853.
14. Chu, H.-A., Babcock, G. T., and Debus, R. J. (2001) in *Proceedings of the 12th International Congress on Photosynthesis*, S13-026, CSIRO Publishing, Collingwood, Australia.
15. Noguchi, T., Inoue, Y., and Tang, X.-S. (1999) *Biochemistry 38*, 10187−10195.
16. Noguchi, T., Inoue, Y., and Tang, X.-S. (1997) *Biochemistry 36*, 14705−14711.
17. Noguchi, T., and Sugiura, M. (2000) *Biochemistry 39*, 10943−10949.
18. Chu, H.-A., Gardner, M. T., O'Brien, J. P., and Babcock, G. T. (1999) *Biochemistry 38*, 4533−4541.
19. Chu, H.-A., Hillier, W., Law, N. A., and Babcock, G. T (2001) *Biochim. Biophys. Acta 1503*, 69−82.
20. Chu, H.-A., Sackett, H., and Babcock, G. T. (2000) *Biochemistry 39*, 14371−14376.
21. Chu, H.-A., Gardner, M. T., Hillier, W., and Babcock, G. T. (2001) *Photosynth. Res. 66*, 57−63.
22. Chu, H.-A., Debus, R. J., and Babcock, G. T. (2001) *Biochemistry 40*, 2312−2316.
23. Hillier, W., and Babcock, G. T. (2001) *Biochemistry 40*, 1503−1509.
24. Noguchi, T., and Sugiura, M. (2001) *Biochemistry 40*, 1497−1502.
25. Noguchi, T., and Sugiura, M. (2002) *Biochemistry 41*, 2322−2330.
26. Noguchi, T., and Sugiura, M. (2002) *Biochemsitry 41*, 15706−15712.
27. Hasegawa, K., Kimura, Y., and Ono, T. (2002) *Biochemistry 41*, 13839−13850.
28. Venyaminov, S. Y., and Kalnin, N. N. (1990) *Biopolymers 30*, 1243−1257.
29. Barth, A. (2000) *Prog. Biophys. Mol. Biol. 74*, 141−173.
30. Rahmelow, K., Hübner, W., and Ackermann, Th. (1998) *Anal. Biochem. 257*, 1−11.
31. Socrates, G. (1994) in *Infrared Characteristic Group Frequencies*, 2nd ed., John Wiley & Sons, Chichester, U.K.
32. Byler, D. M., and Susi, H. (1986) *Biopolymers 25*, 469−487.
33. Haris, P. I., and Chapman, D. (1992) *Trends Biol. Sci. 17*, 328−333.
34. Deacon, G. B., and Phillips, R. J. (1980) *Coord. Chem. Rev. 33*, 227−250.
35. Nara, M., Torii, H., and Tasumi, M. (1996) *J. Phys. Chem. 100*, 19812−19817.
36. Hasegawa, K., Ono, T., and Noguchi, T. (2000) *J. Phys. Chem. B 104*, 4253−4265.
37. Hasegawa, K., Ono, T., and Noguchi, T. (2002) *J. Phys. Chem. A 106*, 3377−3390.
38. Toyama, A., Ono, K., Hashimoto, S., and Takeuchi, H. (2002) *J. Phys. Chem. A 106*, 3403−3412.
39. O'Malley, P. J. (2002) *Biochim. Biophys. Acta 1553*, 212−217.
40. Sugiura, M., and Inoue, Y. (1999) *Plant Cell Physiol. 40*, 1219−1231.
41. Braiman, M. S., Briercheck, D. M., and Kriger, K. M. (1999) *J. Phys. Chem. B 103*, 4744−4750.
42. Nakamura, Y., Kaneko, T., Sato, S., Ikeuchi, M., Katoh, H., Sasamoto, S., Watanabe, A., Iriguchi, M., Kawashima, K., Kimura, T., Kishida, Y., Kiyokawa, C., Kohara, M., Matsumoto, M., Matsuno, A., Nakazaki, N., Shimpo, S., Sugimoto, M., Takeuchi, C., Yamada, M., and Tabata, S. (2002) *DNA Res. 9*, 123−130.
43. Fischer, G., and Wydrzynski, T. (2001) *J. Phys. Chem. B 105*, 12894−12901.
44. Coussan, S., Bouteiller, Y., Perchard, J. P., and Zheng, W. Q. (1998) *J. Phys. Chem. A 102*, 5789−5793.
45. Coussan, S., Alikhani, M. E., Perchard, J. P., and Zheng, W. Q. (2000) *J. Phys. Chem. A 104*, 5475−5483.
46. Hienerwadel, R., Boussac, A., Breton, J., Diner, B. A., and Berthomieu, C. (1997) *Biochemistry 36*, 14712−14723.
47. Rardin, R. L., Tolman, W. B., and Lippard, S. J. (1991) *New J. Chem. 15*, 417−430.

BI0341612